



Contents lists available at ScienceDirect

Spectrochimica Acta Part A: Molecular and Biomolecular Spectroscopy

journal homepage: www.elsevier.com/locate/saa

Solvent effect on the photophysical properties of thermally activated delayed fluorescence molecules

Xiaotong Zhang, Yurong Shi, Lei Cai, Yong Zhou, Chuan-Kui Wang^{*}, Lili Lin^{*}

Shandong Province Key Laboratory of Medical Physics and Image Processing Technology, School of Physics and Electronics, Shandong Normal University, 250014 Jinan, China

ARTICLE INFO

Article history:

Received 24 April 2019

Received in revised form 27 July 2019

Accepted 15 August 2019

Available online 21 August 2019

Keywords:

Thermally activated delayed fluorescence

Solvent effect

Excited state

First-principles

ABSTRACT

As the third-generation organic electroluminescent materials, thermally activated delayed fluorescence (TADF) molecules have become the research focus recently. Significant solvent effect on TADF molecules were found experimentally, while theoretical investigations are quite limited. In this work, the solvent effect on photophysical properties of DCBPY and DTCBPY are investigated with first-principles calculations. The solvent polarity has slight influence on the molecular geometries and orbitals, while it can decrease the energy gap between the first singlet excited state (S1) and first triplet excited state (T1) significantly. Both the oscillator strength and the radiation rates of S1 increase with larger solvent polarity. The large energy gap between S1 and T1 induce negligible inter-system crossing (ISC) and reverse ISC rates between them, which also indicates higher triplet excited states are involved in the up-conversion process. Our results provide valuable information about solvent influence on the light-emitting properties of TADF molecules, which could help one better understand the light-emitting mechanism of them and favor the design of TADF molecules.

© 2019 Elsevier B.V. All rights reserved.

1. Introduction

Extraordinary progress has been made in the development of organic light-emitting diodes (OLEDs) since the new-type high-efficient thermally activated delayed fluorescence (TADF) molecules are reported [1–5]. As the third-generation organic electroluminescent molecular materials, the exciton utilization efficiency of TADF materials with small energy gap between the first singlet excited state (S1) and the first triplet excited state (T1) can reach 100%, which break the limit that the exciton utilization can't exceed 25% in traditional fluorescent materials. A lot of remarkable works have been done on how to realize small S1-T1 energy gap. For example, the general way to decrease the S1-T1 energy gap is to connect electron-donating (D) groups and electron-accepting (A) groups to form D-A molecules or D-A-D molecules [6–8]. Besides, the small S1-T1 energy gap can be realized by connecting D and A groups with a steric hindrance structure, such as twist, bulky, or spirojunction. Some novel design strategies such as combining through-bond and through-space transfer paths or by introducing intramolecular D-A or D-D interaction [9–12], have also been reported. In most TADF systems, significant solvatochromism has been found experimentally [13–15]. Theoretical investigations on the solvent effect on the photophysical properties of TADF molecules are still quite limited [16,18]. Theoretically, excited states with charge transfer (CT) property could be stabilized in a polar solvent¹⁷. The energy gaps

between CT states and localized excited (LE) states may vary in solvents with different polarity [17,18].

In this paper, two donor-acceptor-donor (D-A-D) molecules, (2,5-di(9H-carbazol-9-yl)phenyl)(pyridin-4-yl)methanone (DCBPY) and (3,5-bis(3,6-di-tert-butyl-9H-carbazol-9-yl)-phenyl)(pyridin-4-yl)methanone (DTCBPY) (as shown in Fig. 1) are adopted as the model systems to study the solvent effect on the photophysical properties based on first-principles calculation. In both DCBPY and DTCBPY, two carbazole units and two the *t*-butyl carbazole groups are donors respectively, and they are positioned at *ortho* and *meta* to the pyridine carbonyl moiety (acceptor group). The excited dynamics of these two molecules are also investigated with thermal vibration correlation function (TVCF) method [19–21]. Our theoretical study will provide more insights on the solvent effect on the photophysical properties of TADF molecules, which could help one better understand the light-emitting properties of TADF molecules in solvent.

2. Theoretical methods and computational details

In this paper, the geometry optimization is performed for the ground state (S0) by employing density functional theory (DFT), while the geometry optimization of S1 and T1 are carried out by using the time-dependent density functional theory (TD-DFT). Since the excited states of molecules with D and A units are usually typical CT states, the functional should be chosen prudently. The conventional and popular functional such as B3LYP and PBE0 usually underestimate the excitation energy of CT states due to the low Hartree-Fock percentage (HF%) in

^{*} Corresponding authors.

E-mail addresses: ckwang@sdnu.edu.cn (C.-K. Wang), linll@sdnu.edu.cn (L. Lin).

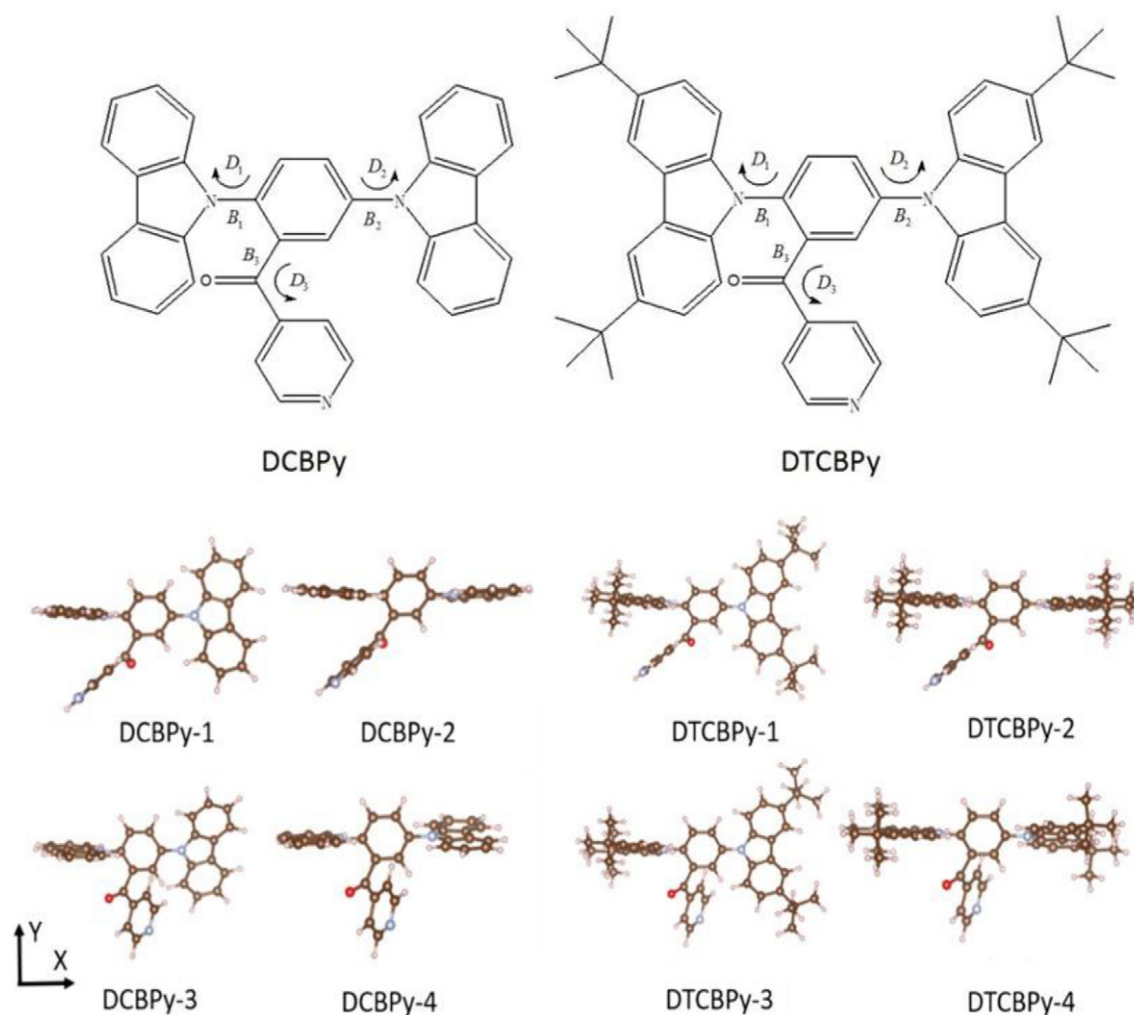


Fig. 1. Geometries of DCBPY and DTCBPY molecules. Bonds and dihedral angles are labeled. Four stable configurations of DCBPY and DTCBPY molecules are shown at the bottom.

them [22–24]. By contrast, the functionals with high HF% would induce excess excitation energy [1,25]. Here we tested several functionals with different HF% and also some functionals with separate short-range and long-range interaction. The absorption and emission spectra calculated with different functionals are investigated (see Supplementary data Table S1). We found that the absorption wavelengths and the emission wavelengths in toluene are quite different when they are calculated with different functionals. It is found that the absorption and emission wavelengths calculated with the PBE0-1/3 functional are 391 nm and 490 nm, which agrees well with experimental values (400 nm and 490 nm). Consequently, the PBE0-1/3 functional is used first, and the 6-31G* basis set is adopted. Solvent polarity effects were taken into account by the polarizable continuum model (PCM) in which both the linear-response (LR) method and the state-specific (SS) method were tested [26–30]. Besides, the frequency calculation for S0 and S1 were performed. Both the vertical excitation energy and the adiabatic excitation energy were calculated respectively and all these calculations were performed using GAUSSIAN 16 package [31].

The excited states dynamics are also studied. There are three decay processes for S1: the radiation process (Fluorescence), the internal conversion (IC) and the ISC. The decay rates are labeled as K_r , K_{IC} and K_{ISC} respectively. In this work, K_r is calculated based on the Einstein spontaneous emission rate formula.

$$K_r = \frac{f \Delta E_{ji}^2}{1.499 \text{ cm}^{-2} \cdot \text{s}} \quad (1)$$

here, f is oscillator strength and ΔE_{ji} is the energy gap between the initial state and the final state with the unit of wave numbers (cm^{-1}). Based on the TVCF method, the non-radiative rate (or IC rate) can be calculated as follows:

$$K_{IC} = \sum_{kl} \frac{1}{\hbar^2} R_{kl} \int_{-\infty}^{\infty} dt \left[e^{i\omega_{ij}t} Z_i^{-1} \rho_{IC}(t, T) \right] \quad (2)$$

here $R_{kl} = \langle \Phi_l | P_{jk} | \Phi_i \rangle \langle \Phi_i | P_{jl} | \Phi_j \rangle$ is the nonadiabatic electronic coupling, Z_i is the partition function and $\rho_{IC}(t, T)$ is the TVCF. One can see the detail information about TVCF method in Refs. [19–21]. The ISC rate was calculated based on classical Marcus rate equation.

$$K_{ISC} = \frac{V_{ji}^2}{\hbar} \sqrt{\frac{\pi}{K_B T \lambda}} \exp \left[-\frac{(\Delta G_{ji} + \lambda)^2}{4 K_B T \lambda} \right] = \frac{V_{ji}^2}{\hbar} \sqrt{\frac{\pi}{K_B T \lambda}} \exp \left[-\frac{\Delta G^\ddagger}{K_B T} \right] \quad (3)$$

here, v_{ji} is the spin-orbit coupling between state i and j . It is calculated with the quadratic response function method in Dalton program [32]. K_B is the Boltzmann constant and T represents the temperature and is set as 298 K. In the activation energy ($\Delta G^\ddagger = \frac{(\Delta G_{ji} + \lambda)^2}{4\lambda}$), ΔG_{ji} and λ are the energy gap and the reorganization energy between state i and j involved. Here the reorganization energy is calculated using adiabatic potential energy surface method (AP) [33,34]. For ISC rate, $\Delta G_{ij} = E_{S1} - E_{Tn}$, and $\Delta G_{ij} = E_{Tn} - E_{S1}$ for reverse ISC (RISC) process. T_n represents the n_{th} triplet excited state.

3. Results and discussion

3.1. Absorption and emission spectra

By performing geometry optimization, we can find that there are four stable configurations for both DCBPy and DTCBPy (shown in Fig. 1). One can see that the surfaces of acceptor groups in both DCBPy-1 and DCBPy-2 are all parallel to the Z axis. The only difference between them is the dihedral angles between two donors. For DCBPy-1, two donors are almost perpendicular. For DCBPy-2, they tend to parallel with each other. For DCBPy-3 and DCBPy-4, the acceptor groups are quite different from that in DCBPy-1 and DCBPy-2. The surfaces of the acceptor groups in DCBPy-3 and DCBPy-4 tend to parallel to the XOY surface. The four configurations for DTCBPy are similar to DCBPy. Based on the energy calculation, the Boltzmann distribution formula is adopted to calculate the population proportions for every configuration (see Supplementary data Table S2). The detail of Boltzmann distribution formula is shown in the Supplementary data. The population proportions for four configurations of DCBPy are 43%, 52%, 3% and 2% respectively. For DTCBPy, they are 44%, 52%, 2% and 2% respectively. It indicates that most DCBPy and DTCBPy molecules almost equally exist in the former two configurations. Consequently, DCBPy-1 and DCBPy-2 as well as DTCBPy-1 and DTCBPy-2 are studied in detail.

The absorption and emission wavelengths of DCBPy-1, DCBPy-2, DTCBPy-1 and DTCBPy-2 in four different solvents (n-hexane, toluene, dichloromethane and tetrahydrofuran) with different polarity are calculated with the PBE0-1/3 functional using the LR-PCM model (see Supplementary data Table S3). We found that both the absorption and emission wavelengths for all the four configurations have little correlation with the solvent polarity, which is quite different from the experimental results. Although LR-PCM/TD-DFT calculation can agree with experimental results well for most systems [35–38], some cautions need to be noticed for some electronics processes characterized by large electron density variation and by a very small oscillator strength, or when a very accurate description of excited state geometry is sought [30,39]. Studies indicated that SS-PCM could provide more balanced description of solvent effects on different excited electronic states than LR-PCM, especially dealing with transitions involving large changes of electron density. SS-PCM/TD-DFT can provide a more accurate treatment of dynamical solvent effects on absorption and emission processes and a more balanced treatment of electronic transitions with very different oscillator strength or with substantial charge transfer (CT) character with respect to traditional LR-PCM/TD-DFT [40,41], though it is more time-consuming than the LR model and may induce some unphysical values [42]. The absorption and emission wavelengths for all the systems calculated with the SS model are also listed in Table S3. It is found that the absorption wavelengths for all the systems change slightly when different solvents are used. Nevertheless, the emission wavelengths of all the systems increase significantly with the polarity increasing, which agree with the trends observed in experiment. One should note that the emission wavelengths of all the systems in more polar solvent are unreasonable, and we think that the SS model may be functional dependent. Recent study indicated that it is necessary to use both the range separate hybrid functional and the SS scheme to study the excited states with large electron rearrangement [43]. The charge density difference between S0 and S1 (T1) of DCBPy-1, DCBPy-2, DTCBPy-1 and DTCBPy-2 in four different solvents can be found in Figs. S1–S4. Large electron rearrangement can be found in all these systems. Then the ω B97XD functional is used, and the absorption and emission wavelengths of all the systems are listed in Table 1. It is found that the absorption wavelengths calculated with the SS-PCM model are also little influenced by solvent polarity. Nevertheless, the emission wavelengths calculated with the SS-PCM method agree with the experimental values. With the polarity increasing, the emission wavelengths show significant red-shift. For comparison, the absorption and emission wavelengths calculated using the LR method are also

Table 1

Absorption and emission wavelengths as well as oscillator strength of S1 calculated with ω B97XD for DCBPy-1, DCBPy-2, DTCBPy-1 and DTCBPy-2 in different solvent.

Configurations	Solvent	λ_{ab-LR} (nm)	λ_{ab-SS} (nm)	λ_{em-LR} (nm)	λ_{em-SS} (nm)	<i>f</i>
DCBPy-1	n-hexane	334	362	401	446	0.022
	Toluene	335	373	404	468	0.025
	THF	335	373	408	581	0.032
	DCM	335	375	409	599	0.032
DCBPy-2	n-hexane	338	362	405	445	0.030
	Toluene	338	373	407	463	0.033
	THF	339	373	413	569	0.043
	DCM	339	375	414	582	0.044
DTCBPy-1	n-hexane	339	368	422	471	0.013
	Toluene	340	378	424	492	0.015
	THF	339	375	426	607	0.022
	DCM	339	377	427	621	0.022
DTCBPy-2	n-hexane	343	369	422	467	0.019
	Toluene	344	380	424	487	0.021
	THF	346	383	430	604	0.022
	DCM	347	385	429	612	0.029

listed, which is in accordance with the results calculated with the PBE0-1/3 functional. Our results indicate that the LR model is not suitable to describe the solvent effect of our systems. The solvent effect investigated with the SS model is more reasonable, while this method is quite functional dependent. Based on the results above, the ω B97XD functional will be adopted in following calculations.

3.2. Solvent effect on geometry structures and electronic structures

The geometry parameters of four configurations in S0 optimized in four kinds of solvents are listed in Supplementary data Table S4. It can be seen that little influence on bond lengths are found for the molecules in different solvents. The dihedral angles change to some extent when the solvents are different. Nevertheless, the changes are no larger than 2 degree, which should be the reason that the absorption wavelength has little dependent on the solvent polarity. The geometry parameters of four systems in S₁ are also listed in Supplementary data Table S5. It is found that the solvent polarity on the geometric parameters are still limited. In view of the significant solvent effect on the emission wavelengths, we deduce that the main effect comes from energy not geometry variation.

The electron distribution and energy levels of the highest occupied molecular orbitals (HOMOs) and the lowest unoccupied molecular orbitals (LUMOs) for four systems in different solvent are shown in Fig. 2. It is found that solvent effect on the HOMO-LUMO energy gaps is not quite significant. With the solvent polarity increasing, the HOMO-LUMO energy gaps have a slight decrease. The energy levels for HOMOs and LUMOs become a little lower when the solvent polarity increases. For all the molecules, electrons in HOMOs are mainly located at two donor groups, while most electrons in LUMOs are distributed on the acceptor group. By analysis of the transition property of the S1 state, we can see that HOMO-LUMO transition shows significant contribution to it. In addition, the HOMO-1 to LUMO transitions also contribute to the S1 states in all the systems (see Supplementary data Table S6). From the electron distribution of HOMO-1, we can see that almost all the HOMO-1s are similar to the HOMOs of the molecule. Consequently, charge transfer property is expected for the S1 state in all the configurations. In addition, solvent polarity has little effect on the energy and electron distribution of molecular orbitals.

3.3. Excited-state properties and decay rates

The energy levels of several low-lying excited states are shown in Fig. 3. All these energy values are calculated based on the S0 geometry. It can be found that there are seven or six triplet excited states with energy lower than S1 for DCBPy-1 and DCBPy-2 in all the solvents. The

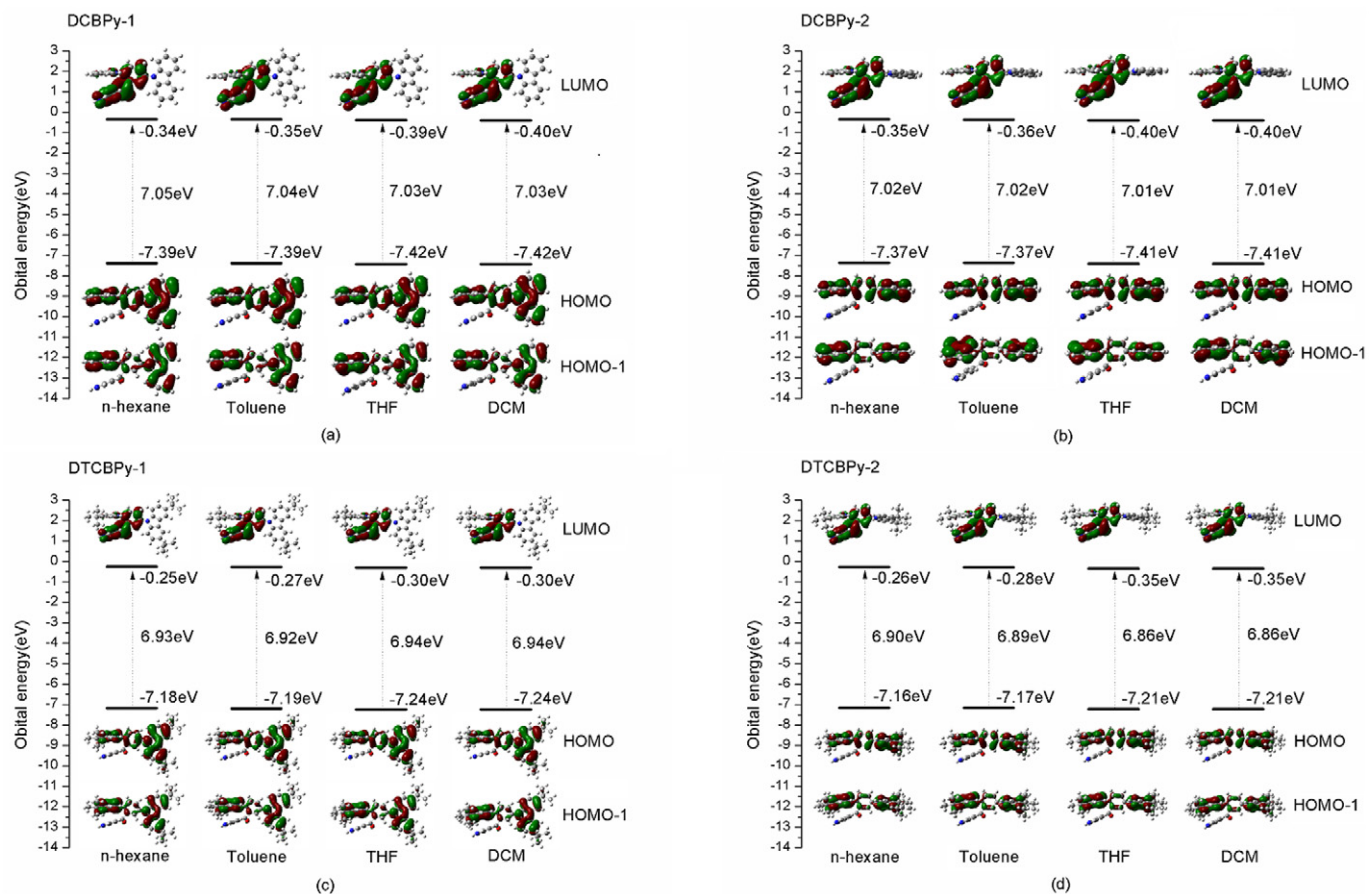


Fig. 2. Electron distribution and energy levels of HOMOs, HOMO-1 s and LUMOs for DCBPy-1 (a), DCBPy-2 (b), DTCBPy-1 (c) and DTCBPy-2 (d) molecules in n-hexane, Toluene, THF and DCM.

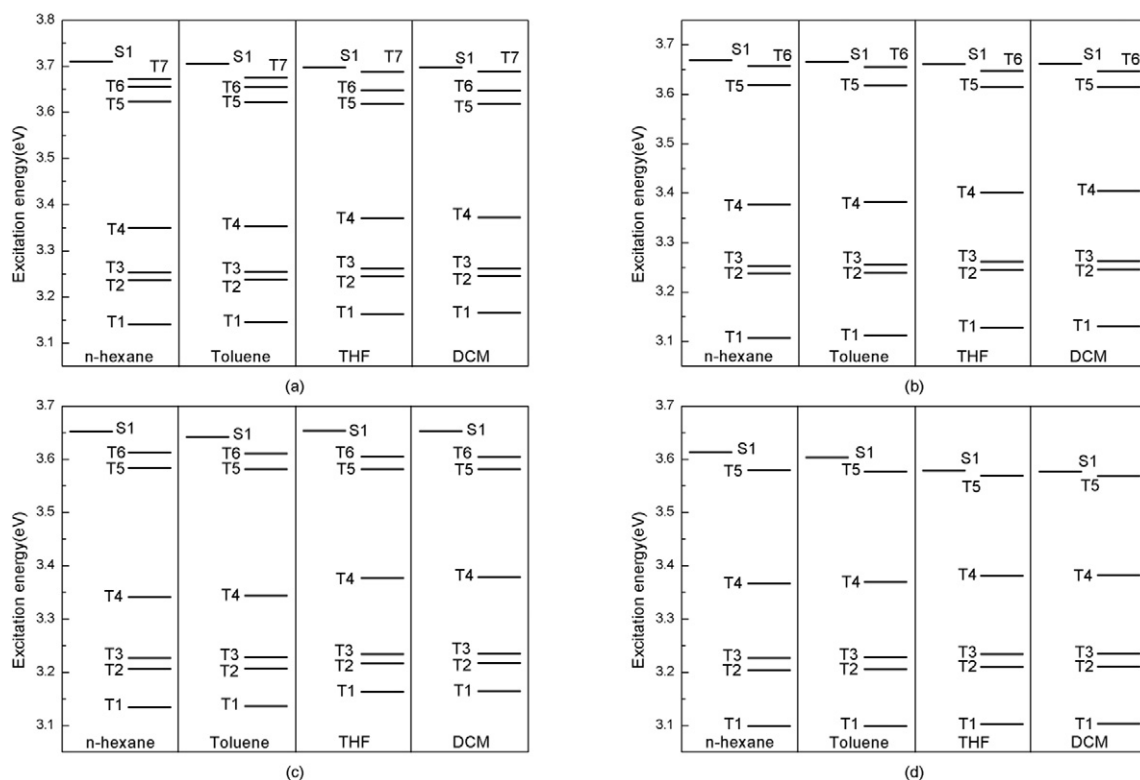


Fig. 3. Energy levels of several low-lying excited states for DCBPy-1 (a), DCBPy-2 (b), DTCBPy-1 (c) and DTCBPy-2 (d) molecules in n-hexane, Toluene, THF and DCM.

Table 2

Radiation rates and nonradiative rates for four conformers. Energy difference, spin-orbit coupling (SOC) and the ISC rates between S1 and T1. The SOC calculated based on the geometry of triplet excited states and reverse ISC (RISC) rate are also listed.

Configurations	Solvent	K_r (s^{-1})	ΔE_{S1-T1} (eV)	K_{IC} (s^{-1})	SOC ^a (cm^{-1})	k_{ISC} (s^{-1})	SOC ^b (cm^{-1})	k_{RISC} (s^{-1})
DCBPy-1	n-hexane	9.0×10^6	0.693	3.18×10^7	0.435	7.99×10^{-5}	0.498	1.05×10^{-4}
	Toluene	1.0×10^7	0.683	5.43×10^7	0.431	1.22×10^{-4}	0.490	1.58×10^{-4}
	THF	1.3×10^7	0.652	3.85×10^7	0.428	4.65×10^{-4}	0.477	5.77×10^{-4}
	DCM	1.3×10^7	0.650	8.74×10^{10}	0.446	5.74×10^{-4}	0.481	6.68×10^{-4}
DCBPy-2	n-hexane	1.2×10^7	0.703	2.74×10^{10}	0.470	3.64×10^{-5}	1.057	1.84×10^{-4}
	Toluene	1.3×10^7	0.695	2.87×10^{10}	0.466	4.99×10^{-5}	1.031	2.45×10^{-4}
	THF	1.7×10^7	0.669	3.72×10^7	0.461	1.95×10^{-4}	1.161	1.24×10^{-3}
	DCM	1.7×10^7	0.666	3.82×10^{10}	0.459	2.18×10^{-4}	1.122	1.30×10^{-3}
DTCBPy-1	n-hexane	4.9×10^6	0.612	6.93×10^8	0.334	1.65×10^{-3}	0.357	1.89×10^{-3}
	Toluene	5.5×10^6	0.605	1.52×10^9	0.343	2.32×10^{-3}	0.350	2.41×10^{-3}
	THF	8.0×10^6	0.577	–	0.349	7.28×10^{-3}	0.344	7.07×10^{-3}
	DCM	8.2×10^6	0.575	2.40×10^9	0.349	7.87×10^{-3}	0.341	7.50×10^{-3}
DTCBPy-2	n-hexane	7.1×10^6	0.633	1.20×10^{11}	0.383	8.65×10^{-4}	0.790	3.68×10^{-3}
	Toluene	7.8×10^6	0.626	1.25×10^{11}	0.387	1.17×10^{-3}	0.799	4.98×10^{-3}
	THF	7.7×10^6	0.602	1.93×10^8	0.395	3.39×10^{-3}	0.788	1.35×10^{-2}
	DCM	1.1×10^7	0.600	7.48×10^{10}	0.391	3.48×10^{-3}	0.793	1.43×10^{-2}

a. SOC between S1 and T1 calculated based on the geometry of S1.

b. SOC between S1 and T1 calculated based on the geometry of T1.

energy of S1 becomes lower when the solvent polarity is increased, while the energy of T1 increases. The S1-T1 energy gap in all four configurations decreases with solvent polarity increasing (see Supplementary data Table S7). The energy gaps between S1-T7 in DCBPy-1 and S1-T5 in DTCBPy-2 are also decreased with the increase of the solvent polarity (see Supplementary data Table S8). For DCBPy-2 and DTCBPy-1, the S1-T6 energy gaps first decrease then becomes higher with solvent polarity increasing.

The S1-T1 energy gap is important value for TADF molecules. The adiabatic S1-T1 energy gaps are also calculated (shown in Table 2), and it is found that the energy gaps between them are all larger than 0.5 eV. So it is difficult for T1 to convert to S1. Nevertheless, triplet excited states lying between S1 and T1 may favor the up-conversion process. The adiabatic S1-T1 energy gaps are a little different from the values calculated with the vertical excitation energy (see Supplementary data Table S7).

The transition properties of S1 and T1 for DCBPy-1 and other configurations are shown in Fig. 4 and Figs. S5–S7 (see Supplementary data). It

is found that all the S1 and T1 states are hybrid local-excited and charge-transfer (HLCT) states. The local excitation (LE) portions of S1 for all systems in all the four solvents are smaller than that for T1. The LE proportion calculated is based on the overlap of two NTOs for the excited states. For the calculation detail, one can refer to Ref. [44]. For all the configurations, the transition for S1 and T1 involves the ortho-donor and the acceptor. The meta-donor has no contribution to the transition of S1 and T1. For all the configurations, the LE component for S1 decreases slightly with increasing solvent polarity, while it increases for T1 to some extent. This slight variation of the transition properties may induce the change of oscillator strengths for S1 and also the photophysical properties.

The oscillator strengths of S1 for all the configurations in different solvents are shown in Table 1. It is found that the oscillator strengths become a little larger when the solvent polarity increases. The values of the oscillator strength of the two conformers for DCBPy and DTCBPy are a little different. The radiation rates of S1 have also slight increase with the polarity increasing, which also have close relationship with

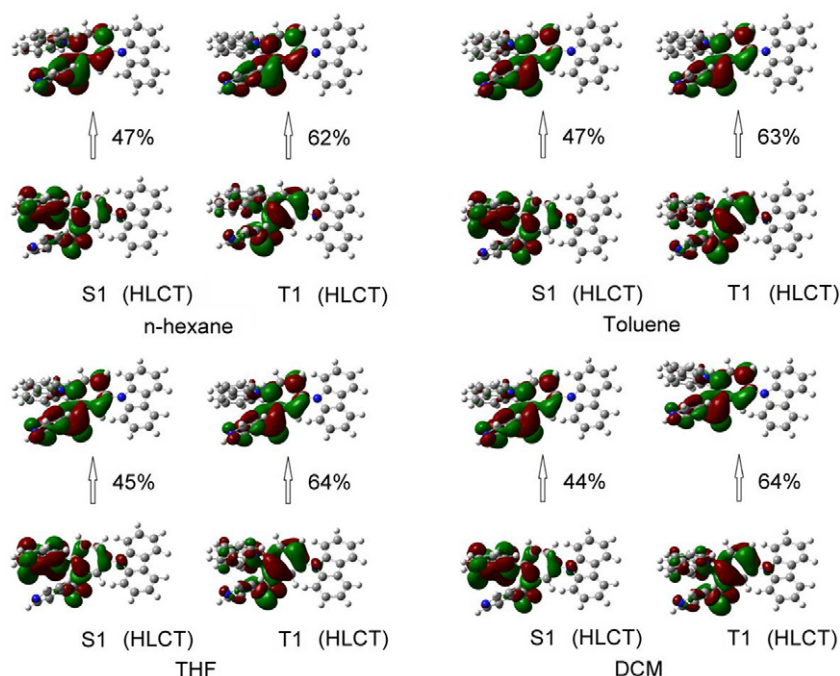


Fig. 4. NTOs for S1 and T1 of DCBPy-1 in n-hexane, Toluene, THF and DCM. The LE proportion for every excited state is also shown.

Table 3

Reorganization energy between S0 and S1 of DCBPY-1, DCBPY-2, DTCBPY-1 and DTCBPY-2 in different solvents. (unit: eV).

Configurations	Solvent	λ_{gs}	λ_{es}	λ_{all}
DCBPY-1	n-hexane	0.32	0.31	0.62
	Toluene	0.32	0.32	0.64
	THF	0.35	0.31	0.66
	DCM	0.35	0.31	0.66
DCBPY-2	n-hexane	0.31	0.30	0.61
	Toluene	0.31	0.30	0.62
	THF	0.34	0.32	0.66
	DCM	0.35	0.32	0.66
DTCBPY-1	n-hexane	0.37	0.35	0.72
	Toluene	0.37	0.35	0.72
	THF	0.41	0.33	0.75
	DCM	0.42	0.33	0.75
DTCBPY-2	n-hexane	0.35	0.33	0.68
	Toluene	0.35	0.33	0.68
	THF	0.36	0.34	0.70
	DCM	0.36	0.33	0.69

the oscillator strength. In addition, the non-radiative rates calculated with TVCF methods are shown in Table 2. It is found that the non-radiative rates for all the molecules are quite large, with the similar orders of magnitude as our former results [45–48]. However, their variation in different solvents seems to have no relationship with the solvent polarity. To check the reasons, the reorganization energy between S1 and S0 is calculated (as listed in Table 3). It is clear that the reorganization energy values between two states of four configurations in four solvents are all larger than 0.6 eV. However, the reorganization energy calculated in our former work is usually smaller than 0.4 eV. Consequently, we think that the TVCF method which based on normal modes analysis may not be appropriate to describe the non-radiative process. That is also why the variation of the non-radiative rates in different solvents are in disorder.

For TADF molecules, the spin orbit coupling (SOC) between S1 and T1 is another important parameter. The S1-T1 SOC values are calculated based on the geometry of S1 and T1 respectively using Dalton program (shown as SOC^a and SOC^b in Table 2). It is found that the values calculated based on S1 are a little smaller than that calculated based on T1. The SOC^a values decreases with increasing solvent polarity in DCBPY, while the SOC^a values increases with increasing solvent polarity for DTCBPY. For all the two molecules, the SOC^b have more complicated variation. With the SOC values and the S1-T1 energy gaps, the ISC rates and the RISC rates can be calculated using the Marcus rates equation (as shown in Table 2). However, the ISC rates and the RISC rates are so small that it indicates that the ISC and RISC processes could not happen between S1 and T1. From the energy structure of several low-lying excited states in Fig. 3, one can deduce that the ISC and RISC processes should happen between S1 and the triplet states close to it.

4. Conclusions

In Summary, the solvent effect on the photophysical properties of the DCBPY and DTCBPY molecules are investigated based on first-principles calculations. Our calculation indicates that the solvent effect cannot be described using the LR-PCM model and the SS-PCM model is more suitable. Nevertheless, the SS-PCM model is quite functional dependent and may induce some unreasonable results at some calculation levels. Our calculation indicates that there are four stable conformers for both DCBPY and DTCBPY molecule. However, the DCBPY-1 and DCBPY-2 as well as DTCBPY-1 and DTCBPY-2 are more stable than other conformers. Based on the results of DCBPY and DTCBPY, we found that the solvent polarity has slight influence on the geometry of S0 and S1 for all the configurations investigated and also the molecular orbitals. Nevertheless, its influence on the excited states and their decay rates are significant. With the solvent polarity increasing, the S1-T1 energy gaps become smaller. The LE component in S1 for all the configurations

decreases slightly, while it increases for T1. The oscillator strength for S1 becomes stronger, which also the main reasons that the radiation gets faster in solvents with larger polarity. The non-radiative rates calculated with the TVCF methods are only reasonable when reorganization energy involved in two states are small enough. The broad S1-T1 energy gaps induce negligible ISC and RISC rates, which also indicates that the up-conversion should happen between S1 and higher triplet excited states.

Acknowledgments

This work is supported by the Shandong Provincial Natural Science Foundation, China (ZR2019MA056) and National Natural Science Foundation of China (Grant Nos. 11874242). Thanks to the supporting of Taishan Scholar Project of Shandong Province. Thanks to the supporting of the Project funded by China Postdoctoral Science Foundation (Grant No. 2018M642689).

Appendix A. Supplementary data

Supplementary data to this article can be found online at <https://doi.org/10.1016/j.saa.2019.117473>.

References

- [1] H. Uoyama, K. Goushi, K. Shizu, H. Nomura, C. Adachi, Highly efficient organic light-emitting diodes from delayed fluorescence, *Nature* 492 (2012) 234–238.
- [2] L.S. Cui, Y.L. Deng, D.P. Tsang, Z.Q. Jiang, Q. Zhang, L.S. Liao, C. Adachi, Controlling synergistic oxidation processes for efficient and stable blue thermally activated delayed fluorescence devices, *Adv. Mater.* 28 (2016) 7620–7625.
- [3] S.Y. Lee, T. Yasuda, H. Komiyama, J. Lee, C. Adachi, Thermally activated delayed fluorescence polymers for efficient solution-processed organic light-emitting diodes, *Adv. Mater.* 28 (2016) 4019–4024.
- [4] Q. Zhang, B. Li, S. Huang, H. Nomura, H. Tanaka, C. Adachi, Efficient blue organic light-emitting diodes employing thermally activated delayed fluorescence, *Nat. Photonics* 8 (2014) 326–332.
- [5] H. Tanaka, K. Shizu, H. Nakanotani, C. Adachi, Twisted intramolecular charge transfer state for long-wavelength thermally activated delayed fluorescence, *Chem. Mater.* 25 (2013) 3766–3771.
- [6] Z. Yang, Z. Mao, Z. Xie, Y. Zhang, S. Liu, J. Zhao, J. Xu, Z. Chi, M.P. Aldred, Recent advances in organic thermally activated delayed fluorescence materials, *Chem. Soc. Rev.* 46 (2017) 915–1016.
- [7] G. Méhes, H. Nomura, Q. Zhang, T. Nakagawa, C. Adachi, Enhanced electroluminescence efficiency in a spiro-acridine derivative through thermally activated delayed fluorescence, *Angew. Chem. Int. Ed. Engl.* 51 (2012) 11311–11315.
- [8] T. Takahashi, K. Shizu, T. Yasuda, K. Togashi, C. Adachi, Donor–acceptor-structured 1,4-diazatriphenylene derivatives exhibiting thermally activated delayed fluorescence: design and synthesis, photophysical properties and OLED characteristics, *Sci. Technol. Adv. Mater.* 15 (2014), 034202.
- [9] X.-L. Chen, J.-H. Jia, R. Yu, J.-Z. Liao, M.-X. Yang, C.-Z. Lu, Combining charge-transfer pathways to achieve unique thermally activated delayed fluorescence emitters for high-performance solution-processed, non-doped blue OLEDs, *Angew. Chem. Int. Ed.* 56 (2017) 15006–15009.
- [10] P. Rajamalli, N. Senthilkumar, P. Gandeepan, P.-Y. Huang, M.-J. Huang, C.-Z. Ren-Wu, C.-Y. Yang, M.-J. Chiu, L.-K. Chu, H.-W. Lin, C.-H. Cheng, A new molecular design based on thermally activated delayed fluorescence for highly efficient organic light emitting diodes, *J. Am. Chem. Soc.* 138 (2016) 628–634.
- [11] Y. Zhang, D. Zhang, M. Cai, Y. Li, D. Zhang, Y. Qiu, L. Duan, Towards highly efficient red thermally activated delayed fluorescence materials by the control of intramolecular π - π stacking interactions, *Nanotechnology* 27 (2016), 094001.
- [12] H. Tsujimoto, D.-G. Ha, G. Markopoulos, H.S. Chae, M.A. Baldo, T.M. Swager, Thermally activated delayed fluorescence and aggregation induced emission with through-space charge transfer, *J. Am. Chem. Soc.* 139 (2017) 4894–4900.
- [13] S. Feuillassre, M. Pauton, L. Gao, A. Desmarchelier, A.J. Riives, D. Prim, D. Tondelier, B. Geffroy, G. Muller, G. Clavier, G. Pieters, Design and synthesis of new circularly polarized thermally activated delayed fluorescence emitters, *J. Am. Chem. Soc.* 138 (2016) 3990–3993.
- [14] W. Ping, Z. Gao, Z. Rong, A. Li, K. Guo, A- π -D- π -a carbazole derivatives with remarkable solvatochromism and mechanoresponsive luminescence turn-on, *J. Mater. Chem. C* 5 (2017) 6136–6143.
- [15] R. Ishimatsu, S. Matsunami, K. Shizu, C. Adachi, T. Imato, Solvent effect on thermally activated delayed fluorescence by 1,2,3,5-tetrakis(carbazol-9-yl)-4,6-dicyanobenzene, *J. Phys. Chem. A* 117 (2013) 5607–5612.
- [16] D. Fan, Y. Yi, Z. Li, W. Liu, Q. Peng, Z. Shuai, Solvent effects on the optical spectra and excited-state decay of triphenylamine-thiadiazole with hybridized local excitation and intramolecular charge transfer, *J. Phys. Chem. A* 119 (2015) 5233–5240.
- [17] H. Sun, Z. Hu, C. Zhong, X. Chen, Z. Sun, J.L. Bredas, Impact of dielectric constant on the singlet–triplet gap in thermally activated delayed fluorescence materials, *J. Phys. Chem. Lett.* 8 (2017) 2393–2398.

- [18] J.M. Mewes, Modeling TADF in organic emitters requires a careful consideration of the environment and going beyond the Franck-Condon approximation, *Phys. Chem. Chem. Phys.* 20 (2018) 12454–12469.
- [19] Y. Niu, W. Li, Q. Peng, H. Geng, Y. Yi, L. Wang, G. Nan, D. Wang, Z. Shuai, MOlecular MAterials Property Prediction Package (MOMAP) 1.0: a software package for predicting the luminescent properties and mobility of organic functional materials, *Mol. Phys.* 116 (2018) 1078–1090.
- [20] Q. Peng, Y. Yi, Z. Shuai, J. Shao, Toward quantitative prediction of molecular fluorescence quantum efficiency: role of Duschinsky rotation, *J. Am. Chem. Soc.* 129 (2007) 9333–9339.
- [21] Y. Niu, Q. Peng, Z. Shuai, Promoting-mode free formalism for excited state radiationless decay process with Duschinsky rotation effect, *Sci. China, Ser. B Chem.* 51 (2008) 1153–1158.
- [22] S.Y. Lee, T. Yasuda, Y.S. Yang, Q. Zhang, C. Adachi, Luminous butterflies: efficient exciton harvesting by benzophenone derivatives for full-color delayed fluorescence OLEDs, *Angew. Chem. Int. Ed.* 53 (2014) 6402–6406.
- [23] K. Kawasumi, T. Wu, T. Zhu, H.S. Chae, T. Van Voorhis, M.A. Baldo, T.M. Swager, Thermally activated delayed fluorescence materials based on homoconjugation effect of donor-acceptor triptycenes, *J. Am. Chem. Soc.* 137 (2015) 11908–11911.
- [24] Y. Sagara, K. Shizu, H. Tanaka, H. Miyazaki, K. Goushi, H. Kaji, C. Adachi, Highly efficient thermally activated delayed fluorescence emitters with a small singlet-triplet energy gap and large oscillator strength, *Chem. Lett.* 44 (2015) 360–362.
- [25] K. Shizu, H. Noda, H. Tanaka, M. Taneda, M. Uejima, T. Sato, K. Tanaka, H. Kaji, C. Adachi, Highly efficient blue electroluminescence using delayed-fluorescence emitters with large overlap density between luminescent and ground states, *J. Phys. Chem. C* 119 (2015) 26283–26289.
- [26] J. Tomasi, B. Mennucci, R. Cammi, Quantum mechanical continuum solvation models, *Chem. Rev.* 105 (2005) 2999–3094.
- [27] R. Improta, UV-visible absorption and emission energies in condensed phase by PCM-TD-DFT methods, in: V. Barone (Ed.), *Computational Strategies for Spectroscopy: From Small Molecules to Nanosystems*, John Wiley & Sons, Chichester, U.K. 2011, pp. 39–76.
- [28] G. Scalmani, M.J. Frisch, B. Mennucci, J. Tomasi, R. Cammi, V. Barone, Geometries and properties of excited states in the gas phase and in solution: theory and application of a time-dependent density functional theory polarizable continuum model, *J. Chem. Phys.* 124 (2006) 427–457.
- [29] R. Improta, V. Barone, G. Scalmani, M.J. Frisch, A state-specific polarizable continuum model time dependent density functional theory method for excited state calculations in solution, *J. Chem. Phys.* 125 (2006), 054103.
- [30] R. Improta, G. Scalmani, M.J. Frisch, V. Barone, Toward effective and reliable fluorescence energies in solution by a new state specific polarizable continuum model time dependent density functional theory approach, *J. Chem. Phys.* 127 (2007), 074504.
- [31] M.J. Frisch, G.W. Trucks, H.B. Schlegel, G.E. Scuseria, M.A. Robb, J.R. Cheeseman, G. Scalmani, V. Barone, G.A. Petersson, H. Nakatsuji, X. Li, M. Caricato, A.V. Marenich, J. Bloino, B.G. Janesko, R. Gomperts, B. Mennucci, H.P. Hratchian, J.V. Ortiz, A.F. Izmaylov, J.L. Sonnenberg, F. Ding Williams, F. Lipparini, F. Egidi, J. Goings, B. Peng, A. Petrone, T. Henderson, D. Ranasinghe, V.G. Zakrzewski, J. Gao, N. Rega, G. Zheng, W. Liang, M. Hada, M. Ehara, K. Toyota, R. Fukuda, J. Hasegawa, M. Ishida, T. Nakajima, Y. Honda, O. Kitao, H. Nakai, T. Vreven, K. Throssell, J.A. Montgomery Jr., J.E. Peralta, F. Ogliaro, M.J. Bearpark, J.J. Heyd, E.N. Brothers, K.N. Kudin, V.N. Staroverov, T.A. Keith, R. Kobayashi, J. Normand, K. Raghavachari, A.P. Rendell, J.C. Burant, S.S. Iyengar, J. Tomasi, M. Cossi, J.M. Millam, M. Klene, C. Adamo, R. Cammi, J.W. Ochterski, R.L. Martin, K. Morokuma, O. Farkas, J.B. Foresman, D.J. Fox, *Gaussian 16 Rev. A*, 03, CT, Wallingford, 2016.
- [32] Dalton, a molecular electronic structure program, Release Dalton 2011 (2011), see <http://daltonprogram.org>.
- [33] V. Lemaire, D.A. da Silva Filho, V. Coropceanu, M. Lehmann, Y. Geerts, J. Piris, M.G. Debije, A.M. van de Craats, K. Senthikumar, L.D.A. Siebbeles, J.M. Warman, J.-L. Brédas, J. Cornil, Charge transport properties in discotic liquid crystals: a quantum-chemical insight into structure–property relationships, *J. Am. Chem. Soc.* 126 (2004) 3271–3279.
- [34] T. Zhang, Y. Jiang, Y. Niu, D. Wang, Q. Peng, Z. Shuai, Aggregation effects on the optical emission of 1,1,2,3,4,5-hexaphenylsilole (HPS): a QM/MM study, *J. Phys. Chem. A* 118 (2014) 9094–9104.
- [35] N.A. Wazzan, Investigation on the performance of PCM/TD-DFT functionals (standard pure, hybrid and long-range corrected) in simulating the absorption and emission spectra of 1-(2,5-dimethylfuran-3-yl)-3-(2,4,5-trimethoxyphenyl)prop-2-en-1-one dye in different solvents, *J. Mol. Struct.* 1164 (2018) 289–296.
- [36] T. Gustavsson, Á. Bányász, E. Lazzarotto, D. Markovitsi, G. Scalmani, M.J. Frisch, V. Barone, R. Improta, Singlet excited-state behavior of uracil and thymine in aqueous solution: a combined experimental and computational study of 11 uracil derivatives, *J. Am. Chem. Soc.* 128 (2006) 607–619.
- [37] F. Santoro, V. Barone, T. Gustavsson, R. Improta, Solvent effect on the singlet excited-state lifetimes of nucleic acid bases: a computational study of 5-fluorouracil and uracil in acetonitrile and water, *J. Am. Chem. Soc.* 128 (2006) 16312–16322.
- [38] R. Improta, V. Barone, Absorption and fluorescence spectra of uracil in the gas phase and in aqueous solution: a TD-DFT quantum mechanical study, *J. Am. Chem. Soc.* 126 (2004) 14320–14321.
- [39] R. Improta, C. Ferrante, R. Bozio, V. Barone, The polarizability in solution of tetraphenyl-porphyrin derivatives in their excited electronic states: a PCM/TD-DFT study, *Phys. Chem. Chem. Phys.* 11 (2009) 4664–4673.
- [40] R. Cammi, S. Corni, B. Mennucci, J. Tomasi, Electronic excitation energies of molecules in solution: state specific and linear response methods for nonequilibrium continuum solvation models, *J. Chem. Phys.* 122 (2005), 104513.
- [41] S. Corni, R. Cammi, B. Mennucci, J. Tomasi, Electronic excitation energies of molecules in solution within continuum solvation models: investigating the discrepancy between state-specific and linear-response methods, *J. Chem. Phys.* 123 (2005), 134512.
- [42] S. Chibani, A. Charaf-Eddin, B. Le Guennic, D. Jacquemin, Boranil and related NBO dyes: insights from theory, *J. Chem. Theory Comput.* 9 (2013) 3127–3135.
- [43] C.A. Guido, B. Mennucci, G. Scalmani, D. Jacquemin, Excited state dipole moments in solution: comparison between state-specific and linear-response TD-DFT values, *J. Chem. Theory Comput.* 14 (2018) 1544–1553.
- [44] R. Chen, Y. Tang, Y. Wan, T. Chen, C. Zheng, Y. Qi, Y. Cheng, W. Huang, Promoting singlet/triplet exciton transformation in organic optoelectronic molecules: role of excited state transition configuration, *Sci. Rep.* 7 (2017) 6225.
- [45] J. Fan, L. Lin, C.-K. Wang, Excited state properties of non-doped thermally activated delayed fluorescence emitters with aggregation-induced emission: a QM/MM study, *J. Mater. Chem. C* 5 (2017) 8390–8399.
- [46] J. Fan, Y. Zhang, Y. Zhou, L. Lin, C.-K. Wang, Excited state properties of a thermally activated delayed fluorescence molecule in solid phase studied by quantum mechanics/molecular mechanics method, *J. Phys. Chem. C* 122 (2018) 2358–2366.
- [47] J. Fan, L. Cai, L. Lin, C.K. Wang, Excited state dynamics for hybridized local and charge transfer state fluorescent emitters with aggregation-induced emission in the solid phase: a QM/MM study, *Phys. Chem. Chem. Phys.* 19 (2017) 29872–29879.
- [48] J. Fan, L. Lin, C.K. Wang, Molecular stacking effect on photoluminescence quantum yield and charge mobility of organic semiconductors, *Phys. Chem. Chem. Phys.* 19 (2017) 30147–30156.